Thermodynamic Analysis of Buoyancy-Induced Flow in Rotating Cavities

J. Michael Owen
Department of Mechanical Engineering,
University of Bath,
BA2 7AY, UK
e-mail: ensjmo@bath.ac.uk

Buoyancy-induced flow occurs in the rotating cavities between the adjacent disks of a gas-turbine compressor rotor. In some cases, the cavity is sealed, creating a closed system; in others, there is an axial throughflow of cooling air at the center of the cavity, creating an open system. For the closed system, Rayleigh–Bénard (RB) flow can occur in which a series of counter-rotating vortices, with cyclonic and anticyclonic circulation, form in the r-ϕ plane of the cavity. For the open system, the RB flow can occur in the outer part of the cavity, and the core of the fluid containing the vortices rotates at a slower speed than the disks: that is, the rotating core "slips" relative to the disks. These flows are examples of self-organizing systems, which are found in the world of far-from-equilibrium thermodynamics and which are associated with the maximum entropy production (MEP) principle. In this paper, these thermodynamic concepts are used to explain the phenomena that were observed in rotating cavities, and expressions for the entropy production were derived for both open and closed systems. For the closed system, MEP corresponds to the maximization of the heat transfer to the cavity; for the open system, it corresponds to the maximization of the sum of the rates of heat and work transfer. Some suggestions, as yet untested, are made to show how the MEP principle could be used to simplify the computation of buoyancy-induced flows. [DOI: 10.1115/1.2988170]

Keywords: rotating cavity, buoyancy, far-from-equilibrium thermodynamics, self-organizing systems, maximum entropy production

1 Introduction

Figure 1 shows a simplified diagram of a high-pressure compressor rotor, through the center of which is an axial flow that is used for cooling purposes in the turbine stages of the gas-turbine engine. This will be referred to here as an *open system*. In some engines, the cavities are sealed, creating rotating annuli, which can be treated as *closed systems*.

For both these systems, buoyancy-induced flow is the principal mechanism for heat transfer from the rotating compressor disks and the peripheral "shrouds," which is the name often used to refer to the outer cylindrical surface of the rotating cavity. In a typical compressor rotor, the centripetal acceleration (which is the dominant acceleration term in the buoyancy force) is several orders of magnitude greater than the gravitational acceleration, and the latter is usually ignored.

Farthing et al. [1] conducted experiments in a rotating-cavity rig, which had an axial throughflow of cooling air and a radius ratio of $a/b \approx 0.1$, and observed a flow structure similar to that shown in Fig. 2. Air entered the cavity in a so-called radial arm, on either side of which was a cyclonic and anticyclonic vortex. The authors used the *linear equations* for an inviscid rotating fluid to show that radial flow can only occur in the rotating core of the fluid if there is a circumferential gradient of pressure. The cyclonic and anticyclonic vortices, similar to those found in the Earth's atmosphere, create regions of low and high pressure, and these provide the Coriolis forces necessary for the radial flow to occur. Laser Doppler Anemometry (LDA) measurements of the air velocity in the rotating cavity revealed that the core rotated at an angular speed, Ω_c, which was slower than that of the disks, Ω. That is, the core of the fluid *slipped* relative to the rotating cavity, and this slip increased as the temperature difference between the heated rotating surfaces and the cooling air increased.

These effects were also observed, experimentally and computationally, by other researchers. Three of the most recent computations were achieved by Sun et al. [2], Bohn et al. [3], and Owen et al. [4]. Sun et al. used large eddy simulation (LES) to compute the flow and heat transfer in a cavity with a central axial throughflow, and they compared their results with available experimental data and with an unsteady Reynolds-averaged Navier–Stokes (RANS) model. The LES model, although computationally demanding, produced better agreement than the RANS model with the measured values of velocity and heat transfer. For both models, computations for a 120 deg segment of the cavity captured the large-scale flow structure and gave similar results to computations for the full 360 deg.

Bohn et al. used an unsteady 3D in-house computational fluid dynamics (CFD) code to compute the flow structure that was observed in an experimental rotating-cavity rig with $a/b=0.3$. (They included a gravitational acceleration in their equations; this provided the nonaxisymmetric term required to trip the initially axisymmetric stratified flow into the Rayleigh–Bénard-type flow discussed below.) Flow visualization in the experimental rig revealed that the flow structure changed periodically with time, and the core could contain one, two, or three pairs of vortices; and, as found in the experiments of Farthing et al., the core slipped. The computed flow structure showed the same periodic behavior as the experimental flow, and the quantitative agreement with the measured oscillation periods was excellent. Figure 3 shows a time sequence of the computed flow structure for $\mathrm{Re}_\phi = 2 \times 10^5$ and $\mathrm{Re}_z = 2 \times 10^4$ where the number of vortex pairs increase from one to two to three; in the subsequent sequence, not shown here, the three pairs reduce to two and then to one again.

Owen et al. [4] compared their computations with the experimental results of Owen and Powell [5]. The experimental results

Contributed by the International Gas Turbine Insititute of ASME for publication in the JOURNAL OF TURBOMACHINERY. Manuscript received January 25, 2008; final manuscript received January 30, 2008; published online March 24, 2010. Review conducted by David Wisler. Paper presented at the ASME Turbo Expo 2007: Land, Sea and Air (GT2007), Montreal, QC, Canada, May 14–17, 2007.

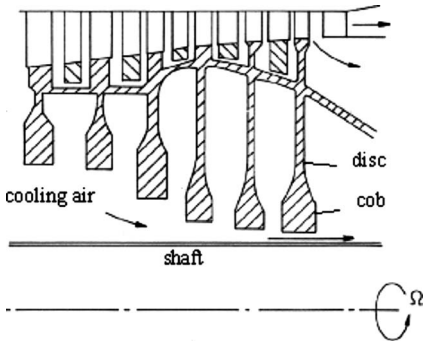

Fig. 1 Simplified diagram of the high-pressure compressor rotor with an axial throughflow of cooling air

were obtained in a rotating-cavity rig with $a/b=0.4$, and LDA measurements suggested that one, two, or three pairs of vortices could occur. A commercial 3D unsteady CFD code (FLUENT) with a k-ε turbulence model (similar to that used in the RANS model of Sun et al.) was used for the computations.

Figure 4 shows the computed temperature contours in the core for two of the test cases, Expt. 2 ($\mathrm{Re}_\phi=0.43\times10^6$ and $\mathrm{Re}_z=0.303\times10^4$) and Expt. 5 ($\mathrm{Re}_\phi=1.57\times10^6$ and $\mathrm{Re}_z=0.164\times10^4$). For Expt. 2, the axial throughflow of the cooling air creates a circular ring of cold fluid (colored blue) at the center of the cavity. "Radial arms" (green) transport some of the fluid from the center to the periphery of the cavity, creating a thin layer of cold air (green) adjacent to the unheated shroud. For Expt. 2, two distinct radial arms are clearly visible, and this is in agreement with the two-cell structure that was observed experimentally. To the right of each radial arm, the circulation is cyclonic, which corresponds to a low-pressure region; in this region, hot air (red) flows axially from the heated disk into the core. To the left of each radial arm, the circulation is anticyclonic, which corresponds to a high-pressure region where the core air flows axially toward the disk. The contours for Expt. 5 are more complex: Several large and small radial arms can be seen and to the right of each one is a high-temperature region. For this case, the LDA measurements were unable to determine the number of cells.

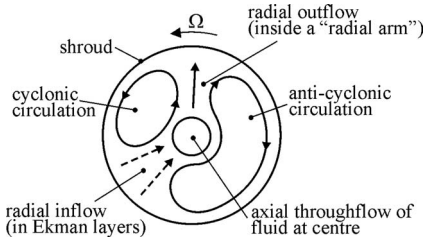

Fig. 2 Schematic of the flow structure in the core of the heated rotating cavity with an axial throughflow of cooling air [1]

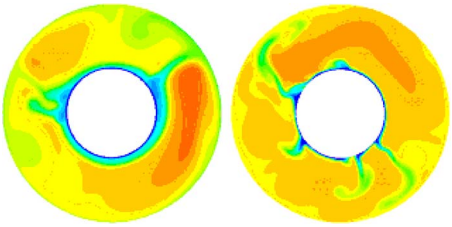

Fig. 4 Computed temperature contours in the core of the heated rotating cavity with an axial throughflow of cooling air [4]. Expt. 2 on the left and Expt. 5 on the right (rotation of the cavity is clockwise).

King et al. [6] used unsteady 2D and 3D CFD codes, with no Reynolds averaging, to compute the heat transfer in a sealed annulus (with $a/b=0.5$) with a radial heat flow from the hot outer cylinder to the cold inner one for $\mathrm{Ra}\leq10^9$. Their computed 2D (r-ϕ) streamlines (see Fig. 5) showed that Rayleigh–Bénard flow occurred, with cyclonic and anticyclonic vortices, in the r-ϕ plane; the vortices could vacillate and their number could change with time. The computed time-average Nusselt numbers were in good agreement with correlations for a stationary cavity but were significantly higher than the correlations of Bohn et al. [7]; the reason for this overestimate of Nu was not understood.

The above papers reveal some of the phenomena associated with buoyancy-induced flow in open and closed rotating cavities, and it is not intended to discuss here the numerous studies of this subject: A comprehensive review is included in Ref. [6]. The reason why vortex pairs occur can be explained by the linear theory referred to above. However, the questions of how many vortex pairs are formed, why, and by how much the core slips, as far as this author knows, have never been addressed. It is the object of this paper to show how thermodynamics can be used to address these questions.

Rayleigh–Bénard flow is an example of a self-organizing system. Such systems, together with the related maximum entropy production principle, are found in the world of far-from-equilibrium thermodynamics, which is discussed in Sec. 2 and which is applied to closed and open rotating cavities in Secs. 3 and 4. In Sec. 5 suggestions are made about how these thermodynamic concepts could be used in CFD, and the main conclusions are summarized in Sec. 6.

Color versions of the figures in this paper can be seen in the electronic version of the paper or in the earlier conference paper (ASME GT2007-27387).

2 Self-Organizing Systems and Maximum Entropy Production

For a background on the thermodynamics used here, the reader is referred to Sonntag and Van Wylen [8] and to Kondepudi and Prigogine [9]. Symbols not defined in the text can be found in the Nomenclature.

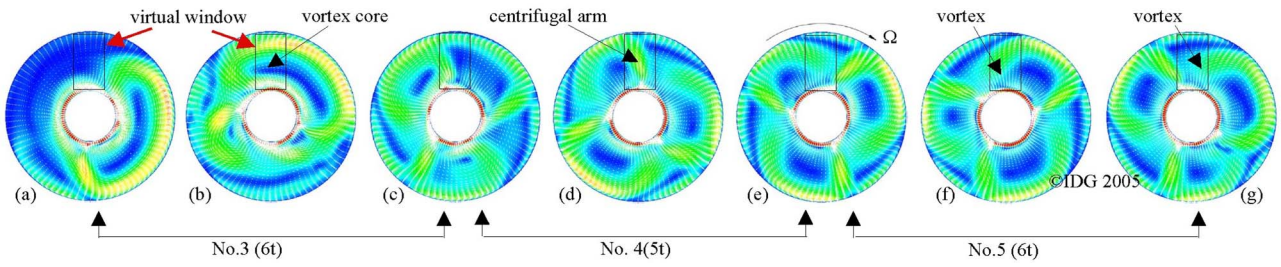

Fig. 3 Computations of the flow structure in the core of the heated rotating cavity with an axial throughflow of cooling air [3]

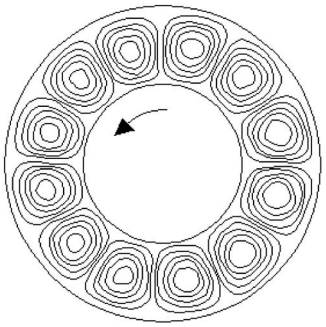

Fig. 5 Computed 2D Rayleigh–Bénard vortices in a sealed rotating annulus [6]

The following common, but not universal, definitions are used below. An *isolated system* is one where neither matter nor energy can cross its boundary; a closed system is where energy, but no matter, can cross the boundary; and an open system is where both matter and energy can cross the boundary.

From the second law of thermodynamics

$$dS_{\text{sys}} + dS_{\text{sur}} \geq 0 \tag{2.1}$$

where the equality holds only for the case of reversible processes. For an isolated system, where there is no transfer of entropy across its boundary, the entropy tends to a maximum, which is reached if thermodynamic equilibrium is achieved.

In nonequilibrium thermodynamics, the rate of entropy production, σ, is a commonly used parameter, where

$$\sigma = \frac{d}{dt}(S_{\text{sys}} + S_{\text{sur}}) \tag{2.2}$$

so that for all irreversible processes $\sigma > 0$. (It should be noted that σ is used here to represent the overall value of entropy production, for the complete system and surroundings, and not the local value that is used in some of the publications cited below.) Self-organizing systems (SOSs) and maximum entropy production (MEP) are two related phenomena that are found in the world of far-from-equilibrium thermodynamics (see, for example, Ref. [10]). These nonlinear systems are associated with instability and fluctuations, and one of the most cited examples is RB convection where the constant flow of heat across the system boundary ensures that the fluid never reaches equilibrium with its surroundings.

Such systems evolve to a quasisteady state that maximizes the rate of entropy exported to the surroundings: high-grade (low entropy) energy enters the system and an equal amount of low-grade (high entropy) energy leaves. The system uses, and maximizes, this flow of energy to organize itself into an optimal state: the higher the rate of energy transfer, the higher the rate of entropy production. (Contrast this with a heat engine for which the designer attempts to maximize the available work output by minimizing the entropy production.) Entropy can be regarded as the waste, or by-product, produced from energy consumption; this waste is exported to the surroundings.

Kondepudi and Prigogine [9] used the term *dissipative structures* for these self-organizing systems. As stated above, the states are created by the dissipation or conversion of high-grade energy into a low-grade form, and Prigogine suggested that the evolution of these states occurs by *order through fluctuations*. (Prigogine was awarded the Nobel Prize for Chemistry in 1977 for his work on dissipative structures. For readers familiar with Prigogine's *minimum entropy production* principle, it should be noted that this principle only applies to linear systems close to equilibrium and not to the nonlinear far-from-equilibrium systems considered here.)

As discussed in Ref. [8], in statistical thermodynamics a *microstate* comprises a particular distribution of all the particles in the system, and each microstate is considered to have an equal probability of existence; a *macrostate* is defined by its observable macroscopic properties, which depend on the constraints on the system. Each possible macrostate can be created from a number of different microstates, and the probability of the existence of each macrostate is related to the number of its possible microstates. This in turn can be related to entropy, defined by Boltzmann in terms of the relative probability of the existence of a particular macrostate. (Boltzmann's constant makes his entropy, which was derived using statistical mechanics, mathematically equivalent to the classical thermodynamics entropy, which is defined in terms of heat and temperature.) Statistical models show that for systems comprising large numbers of particles—as is the case in most engineering applications—a small number of macrostates tend to dominate.

In nonequilbrium statistical thermodynamics, the *paths* rather than *states* are the focus of attention: Micropaths are analogous to microstates, and the most probable macrostate is the one connected by the maximum number of micropaths. Using Shannon's definition of information entropy, Jaynes [11] showed that, away from equilibrium, the most probable macrostates are those associated with the maximum production of entropy. (The introduction of a dimensional constant of proportionality into Shannon's nondimensional information entropy makes it mathematically equivalent to Boltzmann's thermodynamic entropy.) Later, Dewar [12] used Jaynes' statistical approach to show, among other things, that self-organizing systems emerge from the MEP principle.

As discussed by Martyushev and Seleznev [13], the MEP principle has been used extensively in physics, chemistry, and biology. In their comprehensive review, the authors show the relationship between many different applications of the principle, including RB convection and the geophysical systems that are relevant to the work discussed here. They credit Ziegler [14] for having developed the MEP principle for continuum mechanics; his work, which was based on a phenomenological rather than a statistical approach, was largely overlooked by subsequent researchers who developed their own ad hoc applications of the principle.

A review of the MEP principle applied to geophysical systems is given by Ozawa et al. [15]; they compared the Earth's climate system with a heat engine operating between thermal reservoirs at the equator and the poles. In particular, the authors showed how the principle could be applied to RB convection in a stationary system, and their predicted variation of Nusselt numbers with Rayleigh numbers agreed well with experimental correlations.

Paltridge [16–18] was the first to apply an ad hoc version of entropy production to the Earth's climate system; he used a theoretical "zonal average model" in which the oceans and atmosphere were divided into a number of cells connected by a horizontal flow of energy. By assuming that the average annual climate corresponds to the case where the total energy dissipation—and hence the total entropy production—is maximized, he was able to predict annual variations of surface temperature that agreed closely with observations. Although Paltridge's model was initially treated with skepticism by some in the scientific community, many researchers later obtained similar results. The model has since been applied to other areas such as ocean circulation, planetary atmospheres, and global warming. (Using the statistical arguments referred to above, Dewar showed that Paltridge's method was indeed consistent with the MEP principle.)

Of relevance to the discussion of RB flow is the fact that a SOS can often exist in more than one macrostate. In statistical mechanics, an *attractor* is defined as a region of the state-space, or phase-space, that the system can enter but cannot leave (see Ref. [10]). An attractor can be pictured as a landscape with a small number of separate valleys, as shown in Fig. 6, where the depth of the valleys is proportional to σ. Each valley corresponds to a *local* maximum of entropy production, and the deepest valley corresponds to

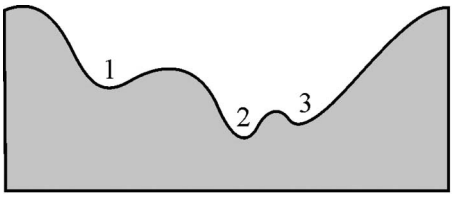

Fig. 6 "Attractor landscape" with three valleys

the *global* maximum. Noise or fluctuations enable the system to move from one valley to another, and a noisy system may move constantly between valleys in a *limit cycle*; the "three-valley" oscillating flow observed by Bohn et al. [3] may well be an example of such a cycle.

These concepts are now applied to buoyancy-induced flow in rotating cavities.

3 Buoyancy-Induced Flow in a Sealed Rotating Annulus

3.1 Entropy Production in a Closed System. A thermodynamic model of a closed rotating cavity is shown in Fig. 7. Heat flows into the fluid inside the cavity from a large hot source (which can be thought of as the outer cylindrical wall of the cavity) and flows from the cavity into a large cold sink (or inner wall), with constant temperatures T_H and T_C, respectively.

There are in effect three subsystems: the source, the cavity, and the sink. If the boundary is drawn around the source and the cavity then the sink can be regarded as the surroundings. If the boundary is drawn around all three then the system can be regarded as isolated. The latter case is chosen here but the final result is the same whichever boundary is chosen. From Eq. (2.2),

$$\sigma = \frac{dS_{\text{cav}}}{dt} + \frac{\dot{Q}_C}{T_C} - \frac{\dot{Q}_H}{T_H} \tag{3.1}$$

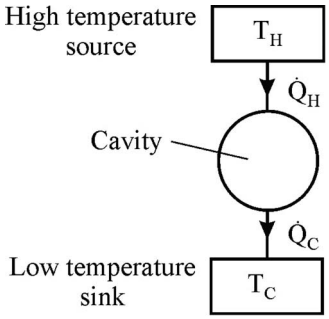

Fig. 7 Thermodynamic model of a closed rotating cavity

In the steady state (if one exists), $\dot{Q}_H = \dot{Q}_C$ and the average temperature and entropy of the fluid in the cavity will be invariant with time, hence

$$\sigma = \dot{Q}_H \frac{T_H - T_C}{T_C T_H} \tag{3.2}$$

For buoyancy-induced flow in rotating cavities, there can be several possible self-organizing macrostates, each corresponding to a particular value of N, the number of vortex pairs. From the above discussion, each macrostate will correspond to a local maximum of σ, which from Eq. (3.2), will correspond to a local maximum of $\dot{Q}_H$.

In the Rayleigh–Bénard convection discussed below, some of the heat entering the cavity is converted to kinetic energy in the vortices, and this energy is then dissipated as heat in the boundary layers before leaving the cavity. That is, low-entropy heat enters the system and high-entropy heat leaves it.

3.2 Rayleigh–Bénard Convection. Lewis [19], Lewis and Rees [20], and King [21] used direct numerical simulation to compute for the 2D unsteady buoyancy-induced laminar flow in a sealed rotating annulus, the temperature of the outer cylindrical surface being T_H and that of the inner surface T_C, where $T_H > T_C$. The initial condition corresponded to a solid-body rotation with axisymmetric radial conduction, and an initial perturbation of the flow field was used to break the symmetry.

Lewis carried out most of his computations for different values of a/b and Ra with a single initial perturbation. The transient development of the initially circular isotherms to the final $N=4$ macrostate (referred to here as N_4) for $\text{Ra}=4\times10^6$ and $a/b=0.5$ is shown in Fig. 8 for four values of τ (where τ, the nondimensional time, is given by $\tau=\alpha t/b^2$). This is a graphic example of the evolution of a self-organizing system.

For the case of $a/b=0.5$ and $\text{Ra}=10^6$, Lewis computed for the transient flow with n point perturbations (where $n=2-8$) at regular circumferential intervals to break the initial symmetry. The resulting values of Nu (which Lewis defined as the ratio of the radial convection to the initial conduction) are shown in Fig. 9. For $n\leq6$ a steady solution exists. For these cases (although it cannot be deduced from Fig. 9) $N=n$, and the maximum value of Nu occurs when $n=N=6$. For $n=N=7$, the flow is unsteady, for $n=8$, the flow is very unsteady, and at $\tau\approx0.5$, the unstable N_8 becomes a stable N_4.

Using the model of the "attractor landscape" discussed above, and shown in Fig. 6, these seven macrostates are all within the attractor, each "valley" of which corresponds to a local maximum in Nu (and hence in σ) with the $n=N=6$ case corresponding to the global maximum. The initial conditions constrained the system to find one of these local valleys from which escape was only possible if the fluctuations were large enough, as was the case for $N=8$. Given sufficiently large fluctuations, the system would be

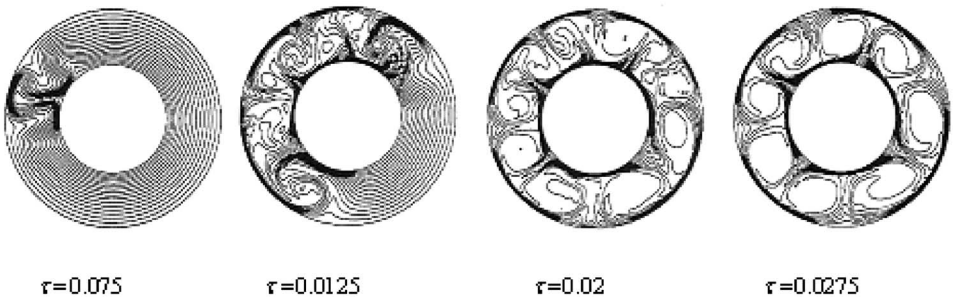

Fig. 8 Transient 2D computed isotherms for a sealed rotating annulus [19]: $a/b=0.5$ and $\text{Ra}=4\times10^6$

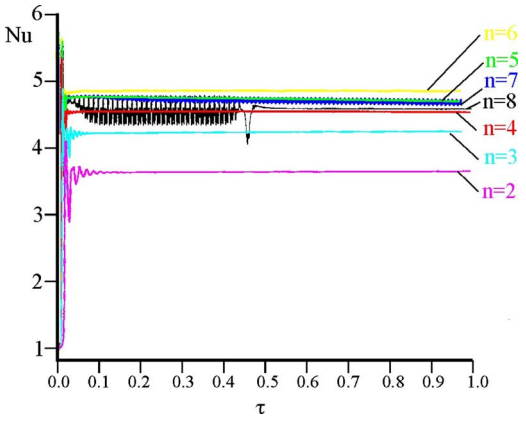

Fig. 9 Effect of *n* on computed Nusselt numbers for a sealed rotating annulus [19]: *a*/*b*=0.5 and Ra=10^6

expected to spend most of the time in the macrostates where Nu and σ are close to the global maximum.

For $10^{3.5}$ Ra$<10^9$, the computations of King (who used a single initial perturbation) showed that, for $a/b=0.5$, N could be 4, 5, or 6 and for $a/b=0.7$, N could be 9, 10, and 11. Although the computations of both King and Lewis showed no systematic effect of Ra on N, they did show that N tends to increase as a/b increases. That is, N increases as the radial height of the cavity, $b-a$, decreases. This suggests that the most probable macrostates are the ones corresponding to the annulus being filled with circular vortices, with the diameter of each vortex being approximately equal to $b-a$. Ignoring the thickness of the boundary layers, the values of a/b that satisfy this "circular-vortex hypothesis" are given by

$$\frac{a}{b}=\frac{2N-\pi}{2N+\pi} \tag{3.3}$$

Figure 10 shows the variation of N with a/b according to Eq. (3.3). Also shown are the values of N computed by King and Lewis for various values of a/b and values of Ra of up to 10^9. It should be noted that the values of N associated with a particular value of a/b could change with time. (This was also observed for open rotating cavities.) Considering the simplicity of this ad hoc

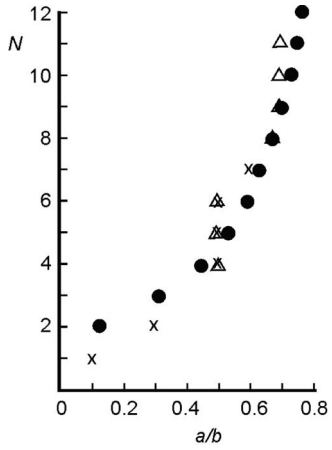

Fig. 10 Variation of the number of vortex pairs, *N*, with the radius ratio, *a*/*b*, of the closed cavity. Solid symbols, Eq. (3.3); *x*, computations of Lewis [19]; and Δ, computations of King [21].

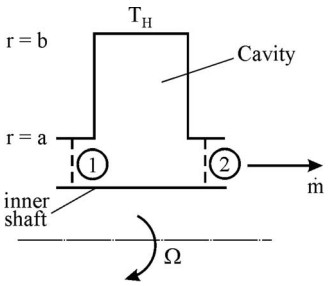

Fig. 11 Simplified diagram of the open rotating cavity

hypothesis, the agreement between Eq. (3.3) and the computations is surprisingly good.

Buoyancy-induced flow in open cavities is discussed below.

4 Buoyancy-Induced Flow in Open Rotating Cavities

Referring to Fig. 11, in the open system a rate of heat transfer, $\dot{Q}_H$, flows into the cavity through the outer cylindrical surface, which has a temperature T_H and a rate of heat transfer, $\dot{Q}_C$, and flows out of the cavity into the axial throughflow of cooling air, which acts as the cold sink.

The cooling air, with a mass flow rate of $\dot{m}$, enters the system with a temperature T_1 and leaves with a higher temperature T_2. Buoyancy effects cause some of this cooling air to be entrained into the rotating cavity (as shown in Fig. 4), and the air consequently leaves the system with an angular momentum higher than that with which it enters. This momentum exchange causes the core of fluid to slip with respect to the disks (as discussed above), which creates a drag on the rotating surfaces. Work must therefore be transferred across the system boundaries to provide the necessary frictional moment.

The analysis below assumes the fluid to be a perfect gas with the following properties:

$$pv=RT \tag{4.1a}$$

$$R=C_p-C_v \tag{4.1b}$$

$$\gamma=\frac{C_p}{C_v} \tag{4.1c}$$

$$dh=C_p\,dT \tag{4.1d}$$

$$ds=C_v\frac{dT}{T}+p\frac{dv}{T} \tag{4.1e}$$

where lowercase symbols are used for the properties v, h, and s to denote their *specific* values. Equation (4.1*e*) can be expressed as

$$ds=C_p\left(\frac{dT}{T}-\frac{\gamma-1}{\gamma}\frac{dp}{p}\right) \tag{4.2}$$

For the steady-state case, Eq. (2.2) can be expressed as

$$\sigma=\dot{m}(s_2-s_1)-\frac{\dot{Q}_H}{T_H} \tag{4.3}$$

and, using Eq. (4.2), it follows that

$$\sigma=\dot{m}C_p\ln\left[\left(\frac{T_2}{T_1}\right)\left(\frac{p_1}{p_2}\right)^{\gamma-1/\gamma}\right]-\frac{\dot{Q}_H}{T_H} \tag{4.4}$$

All quantities evaluated at Stations 1 and 2 in this and subsequent equations should be bulk-average values. When the heat transfer and the temperature of the hot source are nonuniform,

which is usually the case in practice, it is necessary to integrate the local surface temperature T_s and heat flux q_s over the heated surface of the cavity, so that

$$\frac{\dot{Q}_H}{T_H} = \int_A \frac{q_s}{T_s} dA \tag{4.5}$$

where A is the area of the heated surface. This integration, which may also be necessary for the closed cavity discussed above, is easy to achieve from computed results but is more difficult with experimental data.

Further insight can be given by using the first law of thermodynamics for an open system:

$$\dot{Q}_H - \dot{W} = \dot{m} C_p (T_{0,2} - T_{0,1}) \tag{4.6}$$

where $\dot{W}$ is the rate of work done by the system on the surroundings and $T_{0,1}$ and $T_{0,2}$ are the total temperatures at inlet to and outlet from the system. Now

$$\dot{W} = -M\Omega \tag{4.7}$$

where M is the moment exerted by the rotating surfaces on the fluid in the cavity, and

$$M = \dot{m}(r_2 V_{\phi,2} - r_1 V_{\phi,1}) \tag{4.8}$$

Hence, Eq. (4.6) can be expressed as

$$\dot{Q}_H = \dot{m} C_p (T_{0,2} - T_{0,1}) - \dot{m}\Omega (r_2 V_{\phi,2} - r_1 V_{\phi,1}) \tag{4.9}$$

and, from Eq. (4.4),

$$\sigma = \dot{m} C_p \left\{ \ln\left[\left(\frac{T_2}{T_1}\right)\left(\frac{p_1}{p_2}\right)^{\gamma - 1/\gamma} \right] - \frac{1}{T_H}\left[(T_{0,2} - T_{0,1}) - \frac{\Omega}{C_p}(r_2 V_{\phi,2} - r_1 V_{\phi,1}) \right] \right\} \tag{4.10}$$

It is therefore possible to calculate σ using computed, or measured, quantities in the axial throughflow.

For the case when $\delta T \ll T_1$, where $\delta T = T_2 - T_1$,

$$\ln\left(\frac{T_2}{T_1}\right) \approx \frac{\delta T}{T_1} \tag{4.11}$$

In addition, if the pressure and velocity changes are small compared with the temperature changes, Eq. (4.10) reduces to

$$\sigma \approx \dot{Q}_H \frac{T_H - T_1}{T_1 T_H} \tag{4.12}$$

As T_1 for the open system is equivalent to T_C for the closed system, Eq. (4.12) is equivalent to Eq. (3.2).

As for the closed system, the most probable macrostates will be the ones for which σ is maximized, and Eq. (4.10) shows that this will occur when the sum of the rates of heat and work transfer to the system is a maximum. (As discussed in Sec. 2, self-organizing systems tend to maximize the available energy input, importing it as high-grade energy and exporting it in a low-grade form.)

It is convenient to define R_S, the *slip ratio*, as

$$R_S = \frac{\Omega - \Omega_c}{\Omega} \tag{4.13}$$

where Ω_c is the angular speed of the rotating core of fluid in the cavity; in general, $\sigma = \sigma(\dot{Q}_H, R_S)$. The rotational buoyancy force, and therefore $\dot{Q}_H$, increases as the centripetal acceleration of the rotating core ($\Omega_c^2 r$) increases: An increase in R_S is therefore associated with a decrease in $\dot{Q}_H$ and consequently in σ. However, an increase in R_S is also associated with an increase in the frictional work term and in σ. This implies that there are optimum values of R_S and $\dot{Q}_H$ that maximize σ.

Possible ways of using these results to simplify the computation of buoyancy-induced flows are suggested below.

5 Possible Application to CFD

Although buoyancy-induced rotating flows are usually three dimensional and unsteady, in many cases there are quasisteady solutions—or self-organizing macrostates—trying to get out. These metastable macrostates are the ones for which σ is maximized, and the appropriate value of σ can be calculated by Eq. (3.2), Eq. (4.4), or Eq. (4.10). It should be noted, however, that—just as for the experimental measurements—the numerical solutions will depend on the initial conditions and on the fluctuations inside the system and on its boundaries.

If the system oscillates between different macrostates, as observed by Bohn et al. [3], this suggests that the differences in σ, and hence in heat transfer, are relatively small. It should be remembered that Bohn et al. broke the initial axisymmetry of their computed flow by means of a gravitational body force in the equations, which were expressed in a rotating frame of reference. The *vertical* gravitational vector, albeit small in magnitude compared with the centripetal acceleration, rotated relative to the rotating cavity. It is unclear, therefore, whether the observed oscillatory flow was caused by the intrinsic instability of the flow or by the weak oscillatory forcing term.

In principle, it should be possible to use a 3D *steady* CFD code (using, for example, false-transient marching procedures) to find the most probable macrostates. Unless the gravitational term is shown to be significant, the initial symmetry-breaking conditions could be random rather than systematic. Also, the fluctuations—generated by the iterative numerical solution or by the turbulent nature of the flow—need to be sufficiently large to allow σ to achieve its local and global maxima. The sensitivity of a particular macrostate to imposed fluctuations should indicate the stability of the flow and the probable range of Nusselt numbers for that flow.

By using a reference frame that rotates with the fluid core, at angular speed Ω_c, steady computations could be carried out for different values of cavity speed, Ω. This would enable the optimum values of R_S to be determined; this in turn would allow the most probable heat transfer rates to be calculated.

If steady-state solvers were able to produce acceptable solutions then further simplification could be achieved by modeling a segment of the cavity large enough to capture one vortex-pair. Indeed, it might also be possible to make a simple analytical model of such a flow. A steady solution would not be able to capture all the physics but if it were able to provide an acceptable estimate for the heat transfer in an acceptable computational time then the method should be acceptable for design purposes.

The above suggestions are speculative and need to be tested by the CFD community. It is a chicken-and-egg problem: There is insufficient available evidence to test the ideas presented here as no one appears to have applied these thermodynamic concepts to rotating flows. But unless the computationalists and experimentalists search for the evidence they will not find it. The calculation of σ in existing and future computations should show how well the principles apply, and a comparison between steady and unsteady computations should reveal whether or not the above suggestions have merit.

6 Conclusions

For the first time—as far as the author is aware—the principles of far-from-equilibrium thermodynamics have been applied to buoyancy-induced flow in rotating cavities. These flows display the characteristics of self-organizing systems, in which the most probable macrostates are associated with the maximum production of entropy. Equations for σ, the rate of entropy production, have been derived for both closed and open rotating cavities.

The flows that occur in rotating cavities can exist in a number of different metastable macrostates, defined by N, the number of

vortex pairs, and by R_S, the core slip ratio. For closed systems, the maximum value of σ corresponds to the maximum rate of heat transfer; and for open systems, it corresponds to the maximum sum of the rates of heat and work transfer into the cavity.

For the closed cavity, an ad hoc hypothesis was made that circular vortices are more probable than noncircular ones. The predicted variation of N with the radius ratio, a/b, of the cavity agrees well with values computed for a wide range of radius ratios.

The thermodynamic principles used here explain the phenomena that have been observed computationally and experimentally in buoyancy-induced rotating flows. Suggestions—which have yet to be tested numerically—were made to show that it may be possible to use these principles to achieve acceptable estimates of the heat transfer using steady rather than unsteady 3D CFD codes.

There is a paucity of available evidence to test the ideas presented in this paper. It is a chicken-and-egg problem: as no one appears to have applied these principles to rotating flows, there is little published evidence; and unless the computationalists and experimentalists search for the evidence they will not find it.

Acknowledgment

I would like to thank Dr. Tanat Lewis, the results of whose computations were used in this paper, and the reviewers for their helpful comments. I am also indebted to Helen McConville and Mat Sokola who managed to put this paper into the ASME format.

Nomenclature

a = inner radius of the cavity
A = area of the heated surface
b = outer radius of the cavity
C_p = specific heat at constant pressure
C_v = specific heat at constant volume
$\tilde{g}$ = centripetal acceleration
h = specific enthalpy
L = characteristic length
$\dot{m}$ = mass flow rate
M = moment exerted by the rotating surfaces on the fluid in the cavity
n = number of circumferential perturbations
N = number of vortex pairs in the cavity
Nu = Nusselt number
q_s = surface heat flux
Q = heat transferred from the surroundings to the system
$\dot{Q}$ = rate of heat transferred from the surroundings to the system
r = radius
R = gas constant
R_S = slip ratio $(=(\Omega-\Omega_c)/\Omega)$
Ra = Rayleigh number $(=\tilde{g}L^3\beta\Delta T/\alpha^2)$
Re_ϕ = rotational Reynolds number $(=\Omega b^2/\nu)$
Re_z = axial Reynolds number $(=V_z\, b/\nu)$
s = specific entropy
S = entropy
t = time
T = static temperature
T_0 = total temperature
u = specific internal energy
v = specific volume
V_z = bulk-average axial velocity at the inlet to the open cavity
V_ϕ = tangential component of the velocity in a stationary frame
$\dot{W}$ = rate of work done by the system on the surroundings
α = thermal diffusivity
β = volume expansion coefficient
δT = temperature difference
ΔT = characteristic temperature difference
γ = ratio of specific heats
ν = kinematic viscosity
σ = global rate of entropy production
τ = nondimensional time $(=\alpha t/b^2)$
Ω = angular speed of the rotating cavity
Ω_c = angular speed of the rotating core

Subscripts

cav = cavity
C = cold sink
H = hot source
sur = surroundings
sys = system
1 and 2 = inlet and outlet of the open system

References

[1] Farthing, P. R., Long, C. A., Owen, J. M., and Pincombe, J. R., 1992, "Rotating Cavity With Axial Throughflow of Cooling Air: Flow Structure," ASME J. Turbomach., **114**, pp. 237–246.
[2] Sun, X., Linblad, K., Chew, J. W., and Young, C. 2006, "LES and RANS Investigations Into Buoyancy-Affected Convection in a Rotating Cavity With a Central Axial Throughflow," ASME Paper No. GT2006-90251.
[3] Bohn, D., Ren, J., and Tuemmers, C., 2006, "Investigation of the Unstable Flow Structure in a Rotating Cavity," ASME Paper No. GT2006-90494.
[4] Owen, J. M., Abrahamsson, H., and Linblad, K., 2006, "Buoyancy-Induced Flow in Open Rotating Cavity," ASME Paper No. GT2006-91134.
[5] Owen, J. M., and Powell, J., 2006, "Buoyancy-Induced Flow in a Heated Rotating Cavity," ASME J. Eng. Gas Turbines Power, **128**, pp. 128–134.
[6] King, M. P., Wilson, M., and Owen, J. M., 2007, "Rayleigh-Benard Convection in Open and Closed Rotating Cavities," ASME J. Eng. Gas Turbines Power, **129**, pp. 769–777.
[7] Bohn, D., Deuker, E., Emunds, R., and Gorzelitz, V., 1995, "Experimental and Theoretical Investigations of Heat Transfer in Closed Gas Filled Rotating Annuli," ASME J. Turbomach., **117**, pp. 175–183.
[8] Sonntag, R. E., and Van Wylen, G. J., 1982, *Introduction to Thermodynamics: Classical and Statistical*, Wiley, New York.
[9] Kondepudi, D., and Prigogine, I., 1998, *Modern Thermodynamics: From Heat Engines to Dissipative Structures*, Wiley, Chichester, UK.
[10] Heylighen, F., 2002, "The Science of Self-Organization and Adaptivity," *The Encyclopedia of Life Support Systems*, EOLSS, http://ww.eolss.net.
[11] Jaynes, E. T., 1957, "Information Theory and Statistical Mechanics," Phys. Rev., **106**, pp. 620–630.
[12] Dewar, R. L., 2003, "Information Theory Explanation of the Fluctuation Theorem, Maximum Entropy Production and Self-Organized Criticality in Non-Equilibrium Stationary States," J. Phys. A, **36**, pp. 631–642.
[13] Martyushev, L. M., and Seleznev, V. D., 2006, "Maximum Entropy Production Principle in Physics, Chemistry and Biology," Phys. Rep., **426**, pp. 1–45.
[14] Ziegler, H., 1963, "Some Extremum Principles in Irreversible Thermodynamics With Applications to Continuum Mechanics," Rev. Geophys., **4**, pp. 91–193.
[15] Ozawa, H., Ohmura, A., Lorenz, R. D., and Pujol, T., 2003, "The Second Law of Thermodynamics and the Global Climate System: A Review of the Maximum Entropy Production Principle," Rev. Geophys., **41**, 1018.
[16] Paltridge, G. W., 1975, "Global Dynamics and Climate: A System of Minimum Entropy Exchange," Q. J. R. Meteorol. Soc., **101**, pp. 475–484.
[17] Paltridge, G. W., 1978, "The Steady-State Format of Global Climate," Q. J. R. Meteorol. Soc., **104**, pp. 927–945.
[18] Paltridge, G. W., 2001, "A Physical Basis for a Maximum of Thermodynamic Dissipation of the Climate System," Q. J. R. Meteorol. Soc., **127**, pp. 305–313.
[19] Lewis, T. W., 1999, "Numerical Simulation of Buoyancy-Induced Flow in a Sealed Rotating Cavity," Ph.D. thesis, University of Bath, UK.
[20] Lewis, T. W., and Rees, D. A. S., 1996, "Numerical Simulation of Buoyancy-Induced Flows in Sealed Rotating Cavities," Proceedings of the Sixth Australasian Heat and Mass Transfer Conference, Sydney, Australia, Dec. 9–12.
[21] King, M. P., 2002, "Convective Heat Transfer in a Rotating Annulus," Ph.D. thesis, University of Bath, UK.